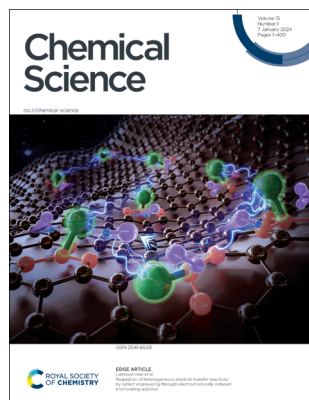


IN THIS ISSUE

ISSN 2041-6539 CODEN CSHCBM 15(1) 1–400 (2024)



Cover
See Lianhuan Han et al., pp. 95–101. Image reproduced by permission of Lianhuan Han from *Chem. Sci.*, 2024, 15, 95.



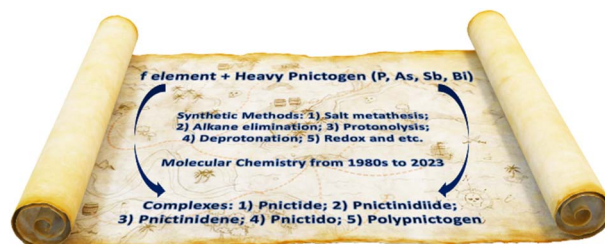
Inside cover
See Diana Portugal Barron and Zhefeng Guo, pp. 46–54. Image reproduced by permission of Diana Portugal Barron and Zhefeng Guo from *Chem. Sci.*, 2024, 15, 46.

REVIEW

13

f-Element heavy pnictogen chemistry

Jingzhen Du, Philip J. Cobb, Junru Ding, David P. Mills* and Stephen T. Liddle*

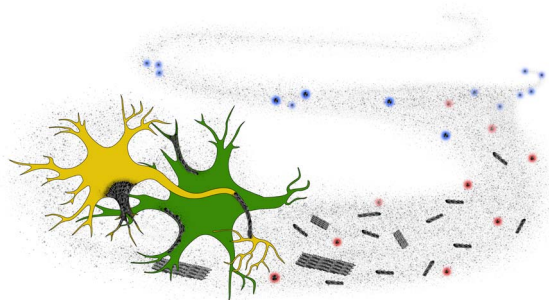


PERSPECTIVES

46

The supersaturation perspective on the amyloid hypothesis

Diana Portugal Barron and Zhefeng Guo*



Royal Society of Chemistry approved training courses

Explore your options.
Develop your skills.
Discover learning
that suits you.

**Courses in the classroom,
the lab, or online**

Find something for every
stage of your professional
development. Search our
database by:

- subject area
- location
- event type
- skill level

Members **get at least 10% off**

Visit rsc.li/cpd-training

**SAVE
10%**

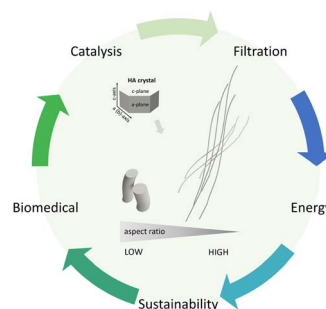


PERSPECTIVES

55

High-aspect-ratio nanostructured hydroxyapatite: towards new functionalities for a classical material

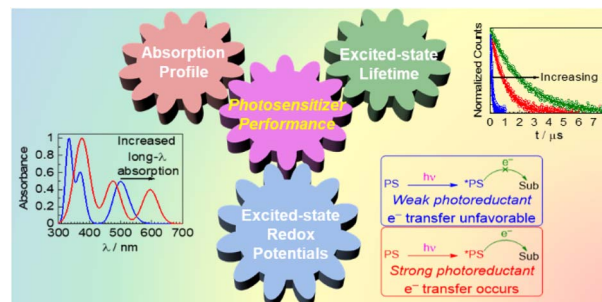
Anna Diez-Escudero, Montserrat Espanol and Maria-Pau Ginebra*



77

Improved transition metal photosensitizers to drive advances in photocatalysis

Dooyoung Kim, Vinh Q. Dang and Thomas S. Teets*

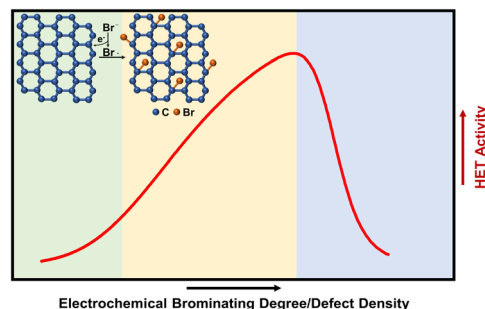


EDGE ARTICLES

95

Regulation of heterogeneous electron transfer reactivity by defect engineering through electrochemically induced brominating addition

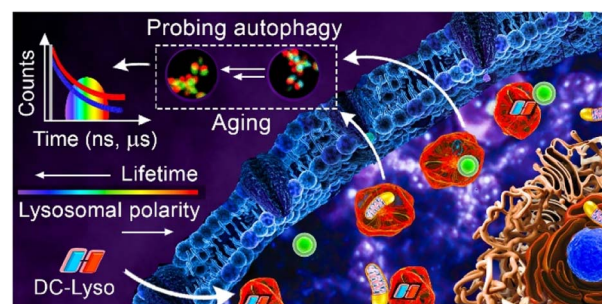
Lanping Zeng, Lianhuan Han,* Wenjing Nan, Weiyong Song, Shiyi Luo, Yuan-Fei Wu, Jian-Jia Su and Dongping Zhan



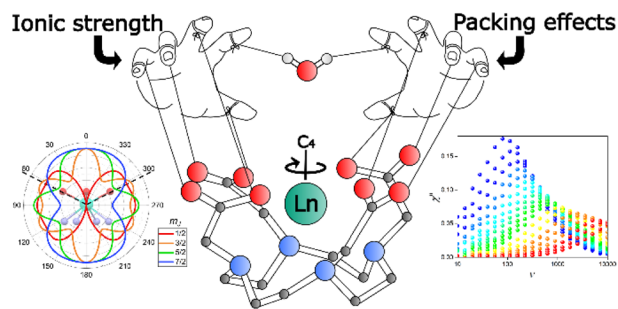
102

Unveiling autophagy and aging through time-resolved imaging of lysosomal polarity with a delayed fluorescent emitter

Subhadeep Das, Abhilasha Batra, Subhankar Kundu, Rati Sharma and Abhijit Patra*



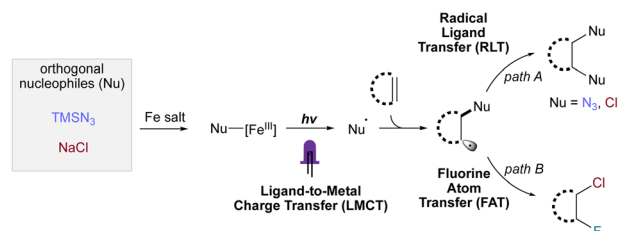
113



LnDOTA puppeteering: removing the water molecule and imposing tetragonal symmetry

Anna Schannong Manvell, Rouven Pflieger, Niels Andreas Bonde, Matteo Briganti,* Carlo Andrea Mattei, Theis Brock Nannestad, Høgni Weihe, Annie K. Powell, Jacques Ollivier, Jesper Bendix* and Mauro Perfetti*

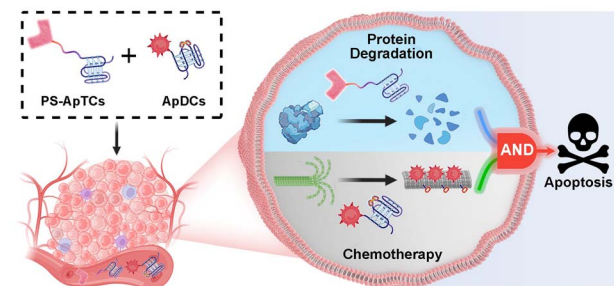
124



Photocatalytic, modular difunctionalization of alkenes enabled by ligand-to-metal charge transfer and radical ligand transfer

Kang-Jie Bian, David Nemoto, Jr, Xiao-Wei Chen, Shih-Chieh Kao, James Hooson and Julian G. West*

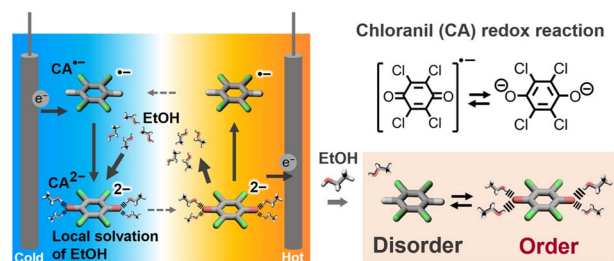
134



Cooperatively designed aptamer-PROTACs for spatioselective degradation of nucleocytoplasmic shuttling protein for enhanced combinational therapy

Ran Liu, Zheng Liu, Mohan Chen, Hang Xing, Penghui Zhang* and Jingjing Zhang*

146




Exploring the local solvation structure of redox molecules in a mixed solvent for increasing the Seebeck coefficient of thermocells

Hirofuka Inoue, Hongyao Zhou,* Hideo Ando, Sakuya Nakagawa and Teppei Yamada*



Photoinduced cerium-catalyzed C–H acylation of unactivated alkanes



unactivated $C(sp^3)-H$ + *benchstable acyl equivalent* $\xrightarrow{\text{OTf}^-}$ *>25 examples*

An atomic surface site interaction point description of non-covalent interactions

The image displays chemical symbols and a molecular model. On the left, a grid of 20 chemical symbols is shown, arranged in 5 rows and 4 columns. The symbols represent the elements H, C, N, O, S, and F, showing their standard single-bonded form and their corresponding Lewis dot structures. The symbols are as follows:

H	C	C	C
N	N	N	N
O	O	O	O
S	S	S	S
F	Cl	Br	I

On the right, a 3D ball-and-stick model of a complex organic molecule is shown. The molecule features a central core with green and yellow spheres, surrounded by a network of gray, red, and blue spheres, representing a complex organic structure.

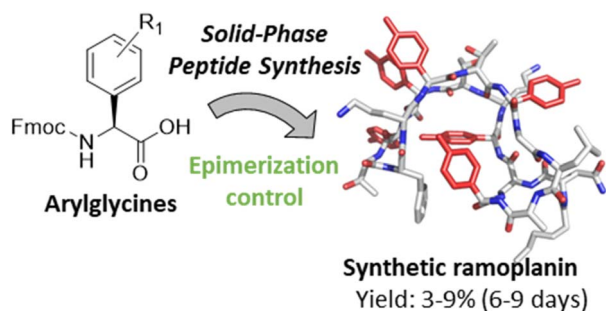
Matrix stiffness-dependent microglia activation in response to inflammatory cues: *in situ* investigation by scanning electrochemical microscopy

The diagram illustrates the signaling pathway for ROS production and cell migration. On the left, a cell is shown on a substrate. A probe (blue cone) is used to apply mechanical stimuli. The probe is labeled 'Substrate stiffness' with red arrows pointing up. This stimulus activates Piezo1 (red channel), which leads to Ca²⁺ release and Rac1 activation. Rac1 then activates NOX2 (blue channel), which produces ROS (red lightning bolt). ROS leads to 'Oxidative Stress' (orange starburst) and also activates LPS (yellow dots). On the right, a cell is shown on a substrate. A probe (blue cone) is used to apply mechanical stimuli. The probe is labeled 'Substrate stiffness/LPS' with red arrows pointing up. This stimulus activates Piezo1 (red channel) and also leads to 'Migration' (blue starburst). The diagram also shows a cell with a nucleus and a red arrow indicating migration.

Dynamic sampling of liquid metal structures for theoretical studies on catalysis

Figure 1 is a plot of Adsorption energy (eV) versus Time (ps). The y-axis ranges from -1.5 to 0.5 eV, and the x-axis ranges from 0 to 40 ps. The plot shows a highly fluctuating black line representing the adsorption energy. A red shaded vertical region between approximately 15 and 20 ps is labeled 'Unfavourable adsorption energy structures'. A blue shaded vertical region between approximately 35 and 40 ps is labeled 'Favourable adsorption energy structures'. Two insets show molecular models of water (red and white spheres) on a Pt surface (gray spheres). The top inset, corresponding to the red shaded region, shows a water molecule in a high-energy, less stable configuration. The bottom inset, corresponding to the blue shaded region, shows a water molecule in a low-energy, more stable configuration.

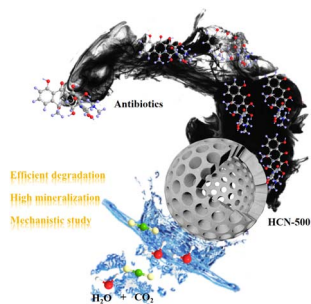
195



Synthetic ramoplanin analogues are accessible by effective incorporation of arylglycines in solid-phase peptide synthesis

Edward Marschall, Rachel W. Cass, Komal M. Prasad, James D. Swarbrick, Alasdair I. McKay, Jennifer A. E. Payne, Max J. Cryle* and Julien Tailhades*

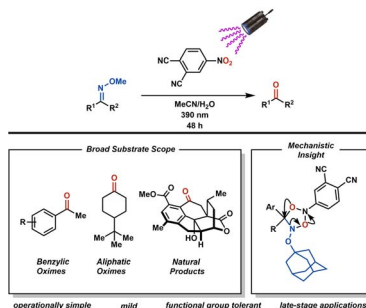
204



Using waste to treat waste: facile synthesis of hollow carbon nanospheres from lignin for water decontamination

Xiang Liu,* Zixuan Hao, Chen Fang, Kun Pang, Jiaying Yan, Yingping Huang, Di Huang* and Didier Astruc*

213

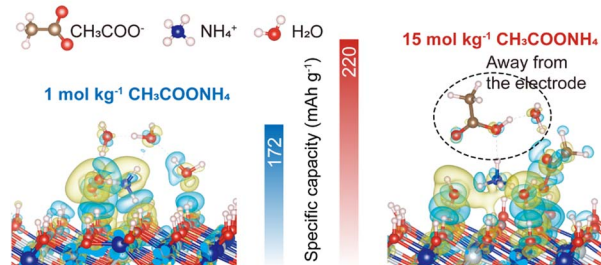


Oxidative cleavage of ketoximes to ketones using photoexcited nitroarenes

Lucas T. Göttemann, Stefan Wiesler and Richmond Sarpong*

220

Solvation structure & Electrochemical performance



A salt-concentrated electrolyte for aqueous ammonium-ion hybrid batteries

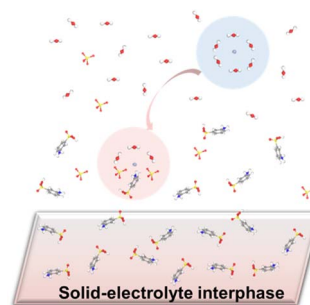
Jianming Meng, Yu Song,* Jing Wang,* Peng Hei, Chang Liu, Mengxue Li, Yulai Lin and Xiao-Xia Liu*



230

Interface regulation of the Zn anode by using a low concentration electrolyte additive for aqueous Zn batteries

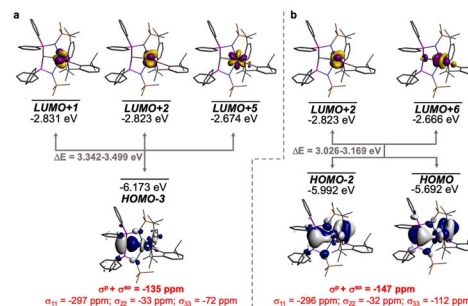
Kuo Wang, Qianrui Li, Guoli Zhang, Shuo Li, Tong Qiu, Xiao-Xia Liu and Xiaoqi Sun*



238

$^{13}\text{C}_{\text{carbene}}$ nuclear magnetic resonance chemical shift analysis confirms $\text{Ce}^{\text{IV}}=\text{C}$ double bonding in cerium(IV)-diphosphonioalkylidene complexes

Cameron F. Baker, John A. Seed, Ralph W. Adams, Daniel Lee* and Stephen T. Liddle*

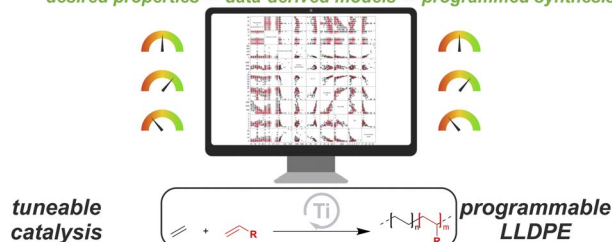


250

Towards designer polyolefins: highly tuneable olefin copolymerisation using a single permethylindenyl post-metallocene catalyst

Clement G. Collins Rice, Louis J. Morris, Jean-Charles Buffet, Zoë R. Turner and Dermot O'Hare*

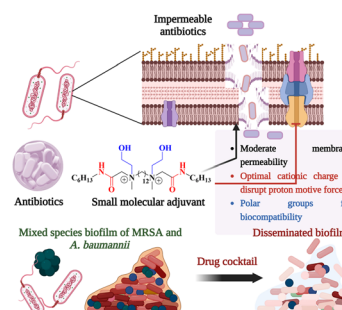
✓ highly active PHENI* Ti catalyst ✓ olefin agnostic
desired properties ⇌ data-derived models ⇌ programmed synthesis



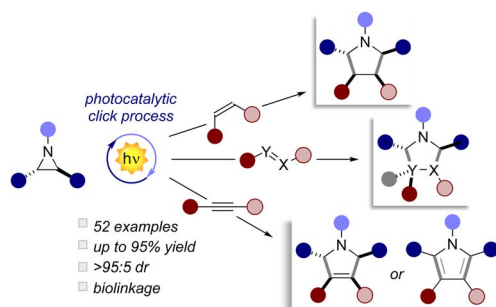
259

Small molecular adjuvants repurpose antibiotics towards Gram-negative bacterial infections and multispecies bacterial biofilms

Rajib Dey, Sudip Mukherjee, Riya Mukherjee and Jayanta Halder*



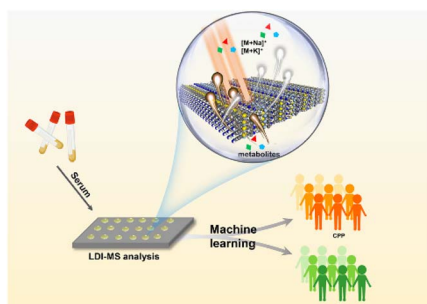
271



Photocatalytic (3 + 2) dipolar cycloadditions of aziridines driven by visible-light

Daniele Mazzarella, Tommaso Bortolato, Giorgio Pelosi and Luca Dell'Amico*

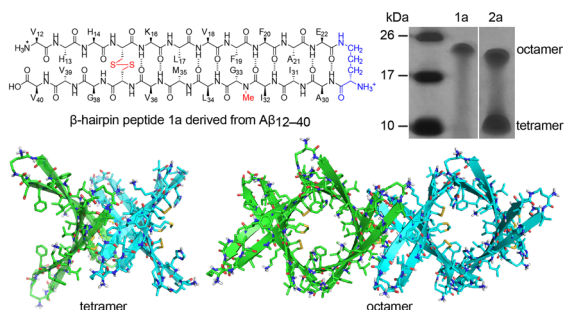
278



Organic metal chalcogenide-assisted metabolic molecular diagnosis of central precocious puberty

Dan Ouyang, Chuanzhe Wang, Chao Zhong, Juan Lin, Gang Xu, Guane Wang* and Zian Lin*

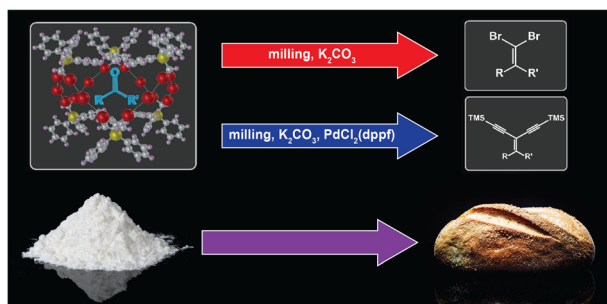
285



A β-barrel-like tetramer formed by a β-hairpin derived from Aβ

Tuan D. Samdin, Chelsea R. Jones, Gretchen Guaglianone, Adam G. Kreutzer, J. Alfredo Freites, Michał Wierzbicki and James S. Nowick*

298



Supramolecular "baking powder": a hexameric halogen-bonded phosphonium salt cage encapsulates and functionalises small-molecule carbonyl compounds

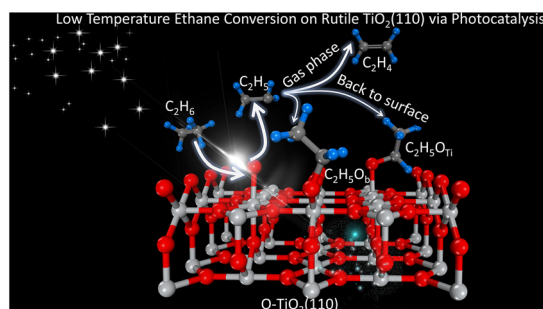
Joseph M. Marrett, Hatem M. Titi, Yong Teoh and Tomislav Friščić*



307

Photocatalytic ethane conversion on rutile $\text{TiO}_2(110)$: identifying the role of the ethyl radical

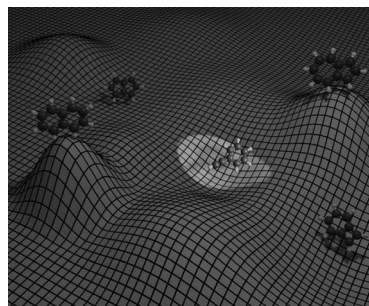
Fangliang Li, Yuemiao Lai, Yi Zeng, Xiao Chen, Tao Wang, Xueming Yang and Qing Guo*



317

New light on the imbroglia surrounding the C_8H_6^+ isomers formed from ionized azulene and naphthalene using ion–molecule reactions

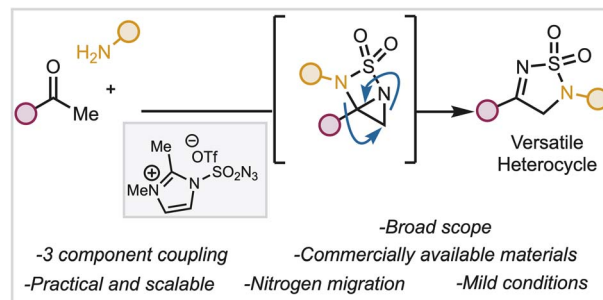
Corentin Rossi, Giel Muller, Roland Thissen, Claire Romanzin, Christian Alcaraz, Sandesh Gondarry, Paul M. Mayer and Ugo Jacovella*



328

Convergent synthesis of thiodiazole dioxides from simple ketones and amines through an unusual nitrogen-migration mechanism

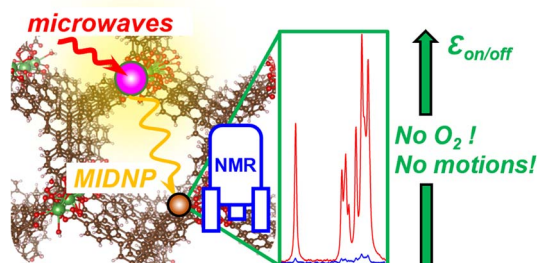
Kunlayanee Punjajom, Paul P. Sinclair, Ishika Saha, Mark Seierstad, Michael K. Ameriks, Pablo García-Reynaga,* Terry P. Lebold* and Richmond Sarpong*



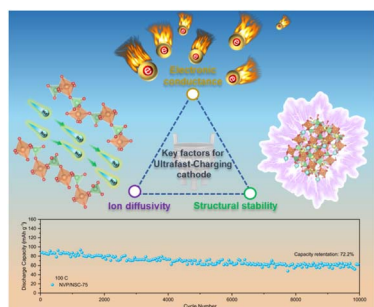
336

Endogenous metal-ion dynamic nuclear polarization for NMR signal enhancement in metal organic frameworks

Ilia B. Moroz, Yishay Feldman, Raanan Carmieli, Xinyu Liu and Michal Leskes*



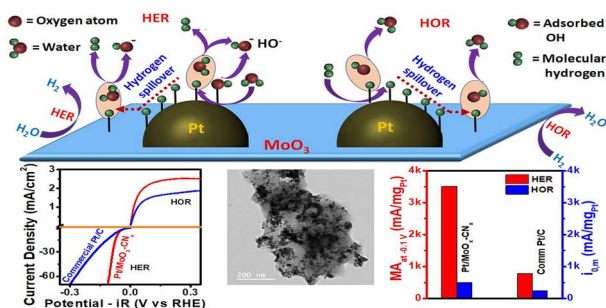
349



Boosting the interfacial dynamics and thermodynamics in polyanion cathode by carbon dots for ultrafast-charging sodium ion batteries

Yujin Li, Yu Mei, Roya Momen, Bai Song, Yujie Huang, Xue Zhong, Hanrui Ding, Wentao Deng, Guoqiang Zou, Hongshuai Hou* and Xiaobo Ji

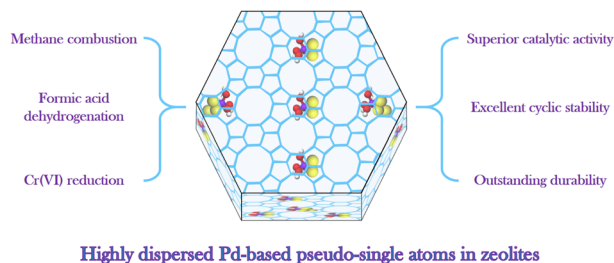
364



Hydrogen spillover enhances alkaline hydrogen electrocatalysis on interface-rich metallic Pt-supported MoO₃

Rajib Samanta, Biplab Kumar Manna, Ravi Trivedi, Brahmananda Chakraborty and Sudip Barman*

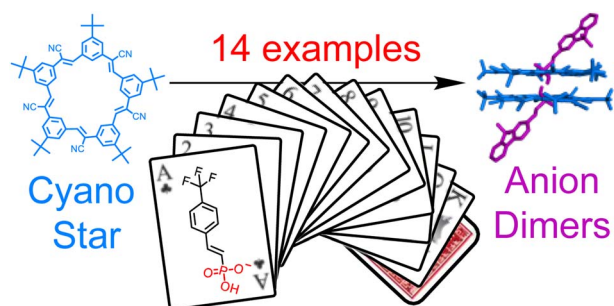
379



Highly dispersed Pd-based pseudo-single atoms in zeolites for hydrogen generation and pollutant disposal

Kai Zhang, Ning Wang,* Yali Meng, Tianjun Zhang, Pu Zhao, Qiming Sun* and Jihong Yu*

389



A library of vinyl phosphonate anions dimerize with cyanostars, form supramolecular polymers and undergo statistical sorting

Yusheng Chen, Anastasia Kuvayskaya, Maren Pink, Alan Sellinger and Amar H. Flood*

